
Chapter
10

Optical Computation

10.1 Introduction

The analysis of an optical system requires a great deal of numerical computation, devoted, for the most part, to the determination of the exact paths taken by light rays as they pass through the system. As previously mentioned, a ray may be traced by the application of Snell's law at each surface. There have been a great variety of formulations devised for raytracing. Early formulas were designed for use with logarithms, and then formulas which were optimized for use with mechanical desk calculators were widely used (the trigonometric equations in Chap. 2 are of this type). Today the most widely used tool for raytracing is the electronic computer, and the equations presented in this chapter are designed for this usage, although they can of course be used with a desk or electronic calculator. These equations do not require that a special computation be carried out for long radii or plane surfaces. They are further characterized by the fact that the quantities involved in them are "bounded," i.e., the maximum size of each term of an equation is readily predicted in terms of the size of the optical system.

The latter sections of the chapter will present detailed directions for computing the numerical values of the aberrations discussed in Chap. 3 and also equations for determining the third-order aberration contributions of surfaces and of thin lenses.

The precision required of an optical calculation is at least six places, obviously depending on the scale of the optical system and the application to which it is put. Trigonometric functions should be carried to at least six places after the decimal; this corresponds to an error of about one-fifth second of arc and is adequate for all but very demanding

applications. For moderate-sized systems, linear dimensions are carried to five- or six-figure accuracy. Very large diffraction-limited systems will, of course, require greater precision throughout. For most calculations, the modern computer (or PC) in single-precision mode is adequate. Double precision is usually used for diffraction and optical path-length calculations.

The time required for an optical computation will obviously depend on the technique and equipment utilized. Tracing a meridional ray (or computing the third-order aberration) through a single surface on a desk calculator is a matter of a minute or so for an experienced operator with a well-thought-out scheme of computation. A skew raytrace is about an order of magnitude more time consuming. The time required on an electronic computer is a matter of fractions of a second on older machines and microseconds on the more powerful machines.

The task presented by raytracing is this: given an optical system defined by its radii, thicknesses, and indices, and a ray defined by its direction and its spatial location, to find the direction and spatial location of the ray after it passes through the system.

Each set of raytracing equations will be presented in four operational sections. First, the “opening” equations, which start the ray into the system; second, the “refraction” equations, which determine the ray direction after passing through a surface; third, the “transfer” equations, which carry the computation to the next surface; and fourth, the “closing” equations, which permit the determination of the final intercept length or height. The refraction and transfer equations are used iteratively, i.e., they are repeated for each surface of the system. The opening and closing equations are used only at the start and finish of the computation. The reader may note that the coordinate system has been changed from that used in the first and second editions of this book, wherein the optical axis was the x axis. The optical axis in this edition is the z axis.

10.2 Paraxial Rays

Although the paraxial raytracing equations were presented in Chap. 2, they are repeated here (in slightly modified form) for completeness.

Opening: 1. Given y and u at the first surface

$$\text{or 2.} \quad y = -lu \quad (10.1a)$$

$$\text{or 3.} \quad y = h - su \quad (10.1b)$$

Refraction:

$$u' = \frac{nu}{n'} + \frac{-cy(n'-n)}{n'} \quad (10.1c)$$

Transfer to the next surface:

$$y_{j+1} = y_j + tu'_j \quad (10.1d)$$

$$u_{j+1} = u'_j \quad (10.1e)$$

Closing:

$$l'_k = \frac{-y_k}{u'_k} \quad (10.1f)$$

or

$$h' = y_k + s'_k u'_k \quad (10.1g)$$

The symbols have the following meanings:

y	the height at which the ray strikes the surface; positive above the axis, negative below.
u	the slope of the ray before refraction.
u'	the slope of the ray after refraction; ray slopes are positive if the ray must be moved clockwise to reach the axis.
h	the height in the object plane at which the ray originates; sign convention same as y .
h'	the height at which the ray intersects the image plane.
l	the distance from the first surface of the system to the axial intercept of the ray; negative if intercept point is to the left of the surface.
l'	the distance from the last surface to the final axial intercept of the ray; positive if the intercept is to the right of the last surface.
s	the distance from the first surface to the object plane; negative if the object plane is to the left of the surface.
s'	the distance from the last surface to the image plane; positive if the image plane is to the right of the surface.
c	the curvature (reciprocal radius) of the surface, equal to $1/R$; positive if the center of curvature is to the right of the surface.
n	the index of refraction preceding the surface.
n'	the index of refraction following the surface.
t	the vertex spacing between surfaces j and $j+1$, positive if surface $j+1$ is to the right of surface j .
n and n'	are positive when the ray travels from left to right, negative when the ray travels from right to left (as it does following a single reflection).
k	subscript indicating the last surface of the system.

The physical meanings of the symbols are indicated in Fig. 10.1.

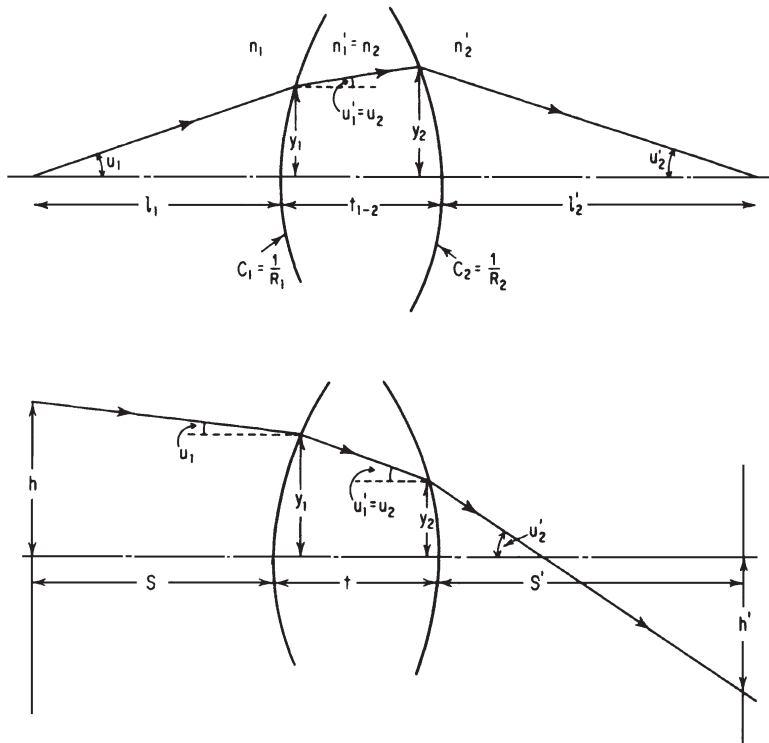


Figure 10.1 Diagrams to illustrate the symbols used in the paraxial ray-tracing equations (10.1a through 10.1g).

10.3 Meridional Rays

Meridional rays are those rays which are coplanar with the optical axis of the system. The plane in which both ray and axis lie is called the meridional plane, and, in an axially symmetrical system, a meridional ray remains in this plane as it passes through the system. The two-dimensional nature of the meridional ray makes it relatively easy to trace. Although a great amount of information about an optical system can be obtained by tracing a few meridional rays plus a Coddington trace or two (Sec. 10.6), given the speed of the modern computer, meridional rays are usually traced as a special case of a skew or general raytrace. However, if rays are to be traced with an electronic pocket calculator, then meridional rays are the obvious choice. The formulas in this section are designed to take advantage of the trigonometric capabilities of this type of calculator.

Opening: 1. Given Q and $\sin U$ at the first surface.

or 2. $Q = -L \sin U$ (10.2a)

or 3. $Q = H \cos U - s \sin U$ (10.2b)

Refraction:

$$\sin I = Qc + \sin U \quad (10.2c)$$

$$\sin I' = \frac{n \sin I}{n'} \quad (10.2d)$$

$$U' = U - I + I' \quad (10.2e)$$

$$Q' = \frac{Q (\cos U' + \cos I')}{(\cos U + \cos I)} \quad (10.2f)$$

Transfer:

$$Q_{j+1} = Q'_j + t \sin U'_j \quad (10.2g)$$

$$U_{j+1} = U'_j \quad (10.2h)$$

Closing:

$$L'_k = \frac{-Q'_k}{\sin U'_k} \quad (10.2i)$$

or

$$H' = \frac{Q'_k + s'_k \sin U'_k}{\cos U'_k} \quad (10.2j)$$

Miscellaneous:

$$y = \frac{Q [1 + \cos (I-U)]}{(\cos U + \cos I)} = \frac{Q' [1 + \cos (I-U)]}{(\cos U' + \cos I')} = \frac{\sin (I-U)}{c} \quad (10.2k)$$

$$z = \frac{Q \sin (I-U)}{(\cos U + \cos I)} = \frac{1 - \cos (I-U)}{c} \quad (10.2l)$$

$$D_{1 \text{ to } 2} = \frac{t - z_1 + z_2}{\cos U'_1} \quad (10.2m)$$

The symbols used are, for the most part, the same as those defined in Sec. 10.2, capitalized to differentiate them from the lowercase paraxial symbols. Symbols new to this section are

Q the distance from the vertex of the surface to the incident ray, perpendicular to the ray; positive if upward.

Q' the distance from the surface vertex to the refracted ray, perpendicular to the ray.

I the angle of incidence at the surface; positive if the ray must be rotated clockwise to reach the surface normal (i.e., the radius).

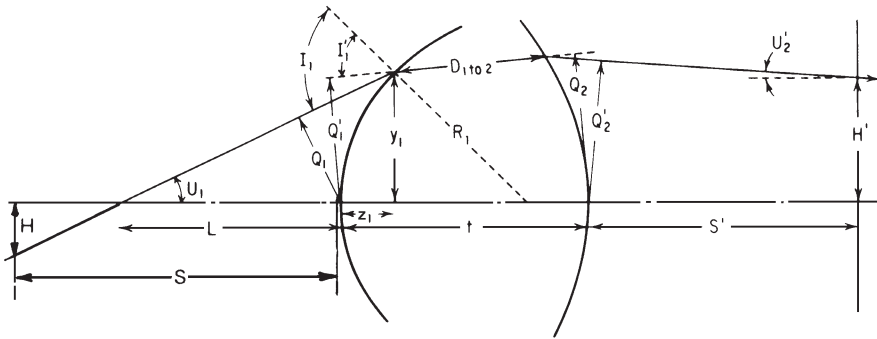


Figure 10.2 Diagram illustrating the symbols used in the meridional raytracing equations.

- I' the angle of refraction.
- z the longitudinal coordinate (abscissa) of the intersection of the ray with the surface; positive if the intersection is to the right of the vertex.
- $D_{1\text{ to }2}$ the distance along the ray between surface 1 and surface 2.

The physical meanings of the symbols are indicated in Fig. 10.2.

Example A

As a numerical example, we will trace a paraxial and a meridional ray through the marginal zone of an equiconvex lens with radii of 50 mm, a thickness of 15 mm, and an index of 1.50. We will trace rays originating at an axial point 200 mm to the left of the first surface and determine the axial intersections for both rays after passing through the lens. We will also determine the height at which the marginal (meridional) ray intersects the paraxial focal plane. Assuming the lens to have an aperture of 40 mm, we will use a value of +0.1 for both the paraxial u and the meridional $\sin U$, so that the ray passes through the lens about 20 mm from the axis.

The following tabulation indicates both the calculation and a convenient way of arranging the raytrace data.

Graphical raytracing (see Fig. 10.3). Meridional rays can be traced using only a scale, straightedge, and compass. The ray is drawn to the surface, and the normal to the surface is erected at the ray-surface intersection. Two circles are drawn about the point of intersection with their radii proportional to n and n' , the refractive indices before and after the surface, respectively. From the intersection of the ray with circle n at point A , a line is drawn parallel with the normal until it intersects circle n' at point B . The refracted ray is then drawn through

Example A—Raytrace Data

R		+50.0		-50.0
$c = 1/R$		+0.020		-0.020
t			15.0	
n	1.00		1.50	1.00

Paraxial Calculation
 given: $u_1 = +0.1$
 $l_1 = -200.0$
 $y_1 = +20.0$ (by 10.1a)

y by 10.1d		+20.0		+19.0
u by 10.1c	+0.1		-0.066667	-0.29
l' by 10.1f				+65.517241

Meridional Calculation
 given: $\sin U_1 = +0.1$
 $L_1 = -200.0$
 $Q_1 = +20.0$ (by 10.2a)

Q	by 10.2g	+20.0		+19.589064
$\sin l$	by 10.2c	+0.5		-0.475278
$\sin I'$	by 10.2d	+0.333333		-0.712918
$\sin U'$	+0.1		-0.083497	-0.372744
$\cos U'$	0.9949874		+0.996508	-0.927934
Q'	by 10.2f	+20.841522		17.008692
L'	by 10.2i			
H' ($s'=l'$)	by 10.2j			+45.631041
				-7.988131

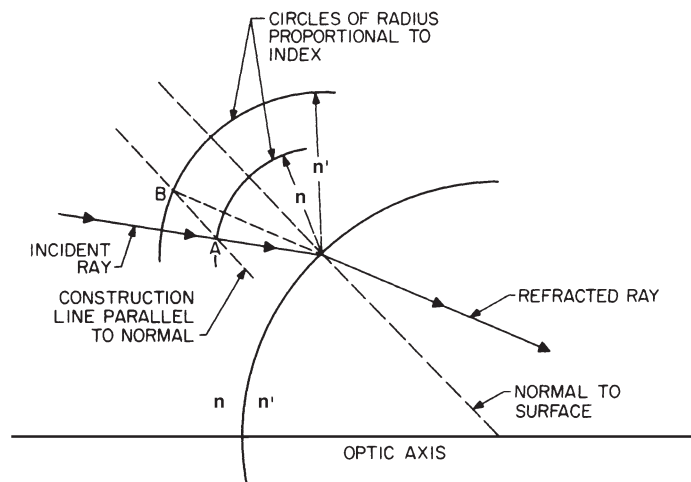


Figure 10.3 Graphical raytrace.

point B and the ray-surface intersection. (For reflection, $n' = -n$, and a single circle is drawn. Point B is located at the intersection of the parallel and the index circle on the *opposite* side of the surface.

If desired, the index circle construction can be carried out off to one side of the drawing (to avoid cluttering the diagram) and the angles transferred to the drawing. An alternative is to measure the angle of incidence and compute the angle of refraction using Snell's law ($n \sin I = n' \sin I'$). The accuracy of graphical raytracing is poor and the process is laborious. Thus, it is rarely used except for crude condenser-type design. It is usually preferable to use a computer and draw the rays from the computed data, or, better yet, to have the computer draw the whole thing.

10.4 General, or Skew, Rays: Spherical Surfaces

A skew ray is a perfectly general ray; however, the application of the term "skew" is usually restricted to rays which are not meridional rays. A skew ray must be defined in three coordinates x , y , and z , instead of just z and y as in the case of meridional rays. Until the advent of the electronic computer, skew rays were rarely traced because of the lengthy computation involved. Since a skew ray takes only a bit longer to trace on an electronic computer than a meridional ray, the reverse situation is now common, and meridional rays are usually traced as special cases of general rays. The general raytracing equations given below are slightly modified from those presented by D. Feder in the *Journal of the Optical Society of America*, vol. 41, 1951, pp. 630–636.

The ray is defined by the coordinates x , y , and z of its intersection point with a surface, and by its direction cosines, X , Y , and Z . The origin of the coordinate system is at the vertex of each surface. Figure 10.4 shows the meanings of these terms. Note that if x and X are both zero, the ray is a meridional ray and direction cosine Y equals $\sin U$. The direction cosines are the projections, on the coordinate axes, of a unit-length vector along the ray. The direction cosines may be visualized as the length, height, and width of a rectangular solid or box which has a diagonal equal to one (1.0). (Note that the *optical* direction cosine is simply the direction cosine as defined above, multiplied by the index of refraction.)

The computation is opened by determining the values for x , y , z , X , Y , and Z with respect to an arbitrarily chosen reference surface, which may be plane (the usual choice) or spherical. Convenient choices for the location of the reference surface are at the object (which allows the easy use of a curved object surface, if appropriate), at the vertex of the

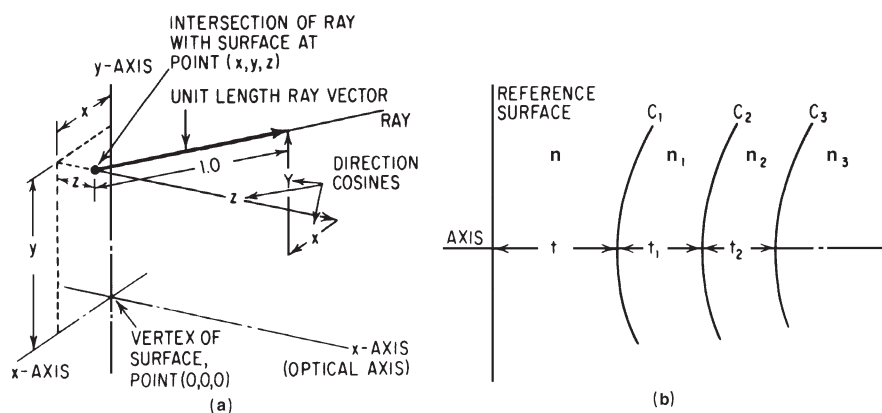


Figure 10.4 Symbols used in skew raytracing Eqs. 10.4a through 10.4p. (a) The physical meanings of the spatial coordinates (x, y, z) of the ray intersection with the surface and of the ray direction cosines, $X, Y,$ and Z . (b) Illustrating the system of subscript notation.

first surface, or at the entrance pupil. Note that Eq. 10.3a is simply the equation of a sphere (and thus assures that the ray origin point lies in the reference surface), and that Eq. 10.3b assures that the square of the unit vector along the ray is equal to 1.0.

Opening (at the reference surface):

$$c(x^2 + y^2 + z^2) - 2z = 0 \quad (10.3a)$$

$$X^2 + Y^2 + Z^2 = 1.0 \quad (10.3b)$$

Transfer to the first (or next) surface:

$$e = tZ - (xX + yY + zZ) \quad (10.3c)$$

$$M_{1z} = z + eZ - t \quad (10.3d)$$

$$M_1^2 = x^2 + y^2 + z^2 - e^2 + t^2 - 2tz \quad (10.3e)$$

$$E_1 = \sqrt{Z^2 - c_1(c_1 M_1^2 - 2M_{1z})} \quad (10.3f)$$

$$L = e + \frac{(c_1 M_1^2 - 2M_{1z})}{Z + E_1} \quad (10.3g)$$

$$z_1 = z + LZ - t \quad (10.3h)$$

$$y_1 = y + LY \quad (10.3i)$$

$$x_1 = x + LX \quad (10.3j)$$

Refraction:

$$E' = \sqrt{1 - \left(\frac{n}{n_1}\right)^2 (1 - E_1^2)} \quad (10.3k)$$

$$g_1 = E'_1 - \frac{n}{n_1} E_1 \quad (10.3l)$$

$$Z_1 = \frac{n}{n_1} Z - g_1 c_1 z_1 + g_1 \quad (10.3m)$$

$$Y_1 = \frac{n}{n_1} Y - g_1 c_1 y_1 \quad (10.3n)$$

$$X_1 = \frac{n}{n_1} X - g_1 c_1 x_1 \quad (10.3o)$$

Terms without subscript refer to the reference surface and the following space. Terms subscripted with 1 refer to the first surface and the following space.

The symbols have the following meanings:

x, y, z	The spatial coordinates of the ray intersection with the reference surface.
x_1, y_1, z_1	The spatial coordinates of the ray intersection with surface #1.
M_1	The distance (vector) from the vertex of surface #1 to the ray, perpendicular to the ray.
M_{1z}	The z component of M_1 .
E_1	The cosine of the angle of incidence at surface #1.
L	The distance along the ray from the reference surface (x, y, z) to surface #1 (x_1, y_1, z_1). L_j is the distance from surface j to $j+1$.
E'_1	The cosine of the angle of refraction (I') at surface #1.
X, Y, Z	The direction cosines of the ray in the space between the reference surface and surface #1 (before refraction).
X_1, Y_1, Z_1	The direction cosines after refraction by surface #1.
c	The curvature (reciprocal radius = $1/R$) of the reference surface.
c_1	The curvature of surface #1.
n	The index between the reference surface and surface #1.
n'	The index following surface #1.
t	The axial spacing between the reference surface and surface #1.

Notice that the choice of the positive value for the square root in Eq. 10.3f selects that intersection of the ray with the surface which is nearer the surface vertex. Also, if the argument under the radical in Eq. 10.3f is negative, it indicates that the ray misses (never intersects) the spherical surface. If the argument under the radical in Eq. 10.3k is negative, it indicates that the angle of incidence exceeds the critical

angle; the ray is thus subject to total internal reflection (TIR) and cannot pass through the surface.

The calculation is opened by inserting c , two of the coordinates (x, y, z) , and two of the direction cosines (X, Y, Z) into Eqs. 10.3a and b and solving for the third coordinate and the third direction cosine. Then the intersection of the ray with the first surface (x_1, y_1, z_1) is determined from Eqs. 10.3c through 10.3j. Next the ray direction cosines after refraction at surface #1 (X_1, Y_1, Z_1) are found from Eqs. 10.3k through 10.3o. This completes the raytrace through the first surface; at this point Eqs. 10.3a and 10.3b (with unit subscripts) may be used to check the accuracy of the computation.

To transfer to the second surface, the subscripts of Eqs. 10.3c through 10.3j are advanced by one, and $x_2, y_2,$ and z_2 are determined. Similarly, the direction cosines after refraction (X_2, Y_2, Z_2) at surface #2 are found by Eqs. 10.3k through 10.3o with the subscripts incremented.

This process is repeated until the intersection of the ray with the final surface of the system, which is usually the image plane, has been determined. This completes the calculation.

Note that any ray which intersects the axis is a meridional ray; thus it is only necessary to trace skew rays from off-axis object points. Further, there is no loss of generality in assuming that the object point lies in the $y-z$ plane of the coordinate system (because we assume a system with axial symmetry). Therefore, any skew ray can be started with x equal to zero. When this is done, it is apparent that the two halves of the optical system, in front of, and behind the $y-z$ plane are mirror images of each other and that any ray X_k, Y_k, Z_k passing through x_k, y_k, z_k has a mirror image $(-X_k), Y_k, Z_k$ passing through $(-x_k), y_k, z_k$ in the other half of the system. For this reason, it is only necessary to trace skew rays through one-half of the system aperture; rays through the other half are represented by the same data with the signs of x and X reversed.

Example B

Using the lens of Example A, we will trace a skew ray originating in the object plane (200 mm to the left of the lens) at a point 20 mm above the axis. Thus, the ray intersection coordinates in the reference plane (in this case, the object plane) are $x = 0, y = +20, z = 0$. If we set $Y = -0.1$ and $X = +0.1$, the ray will intersect the first surface of the lens approximately in the $x-z$ plane, about 20 mm in front of the (optical) z axis. For the image surface we will use the paraxial focal plane as computed in Example A. The calculation is shown in the table on the next page.

Example B—Skew Trace through a Sphere

	Object plane	First surface	Second surface	Image plane
<i>R</i>		+50	-50	
<i>c</i>	0.0	+0.02	-0.02	0.0
<i>t</i>		+200.	+15.	+65.517241
<i>n</i>		1.0	1.50	1.0
Transfer:				
<i>e</i> by 10.3c		+199.989899	+12.188013	+71.860665
<i>M_z</i> by 10.3d		-2.0201011	+1.590643	-3.468077
<i>M²</i> by 10.3e		+404.040418	+389.369720	107.475746
<i>E</i> by 10.3f		+0.8588247	+0.8772472	+0.9224280
<i>L</i> by 10.3g		+206.546141	+6.327736	+75.620392
<i>z</i> by 10.3h	(0.0)	+4.470247	-4.237125	0.000000
<i>y</i> by 10.3i	(+20.0)	-0.654614	-1.046031	-7.078610
<i>x</i> by 10.3j	(0.0)	+20.654614	+20.116291	-8.456088
Refraction:				
<i>E'</i> by 10.3k		+0.9398771	+0.6939135	
<i>g</i> by 10.3l		+0.3673272	-0.6219573	
<i>Z</i> by 10.3m	(+0.9899495)	+0.9944527	+0.9224280	
<i>Y</i> by 10.3n	(-0.1)	-0.0618575	-0.0797745	
<i>X</i> by 10.3o	(+0.1)	-0.0850734	-0.3778396	
Check:				
zero by 10.3a	(0.0)	+0.0000001	-0.0000015	
1.0 by 10.3b	(1.0)	1.0000000	1.0000001	

10.5 General, or Skew, Rays: Aspheric Surfaces

For raytracing purposes, an aspheric surface of rotation is conveniently represented by an equation of the form

$$z = f(x, y) = \frac{cs^2}{[1 + \sqrt{1 - c^2s^2}]} + A_2s^2 + A_4s^4 + \dots + A_js^j \quad (10.4a)$$

where *z* is the longitudinal coordinate (abscissa) of a point on the surface which is a distance *s* from the *z* axis. Using the same coordinate system as Sec. 10.4, the radial distance *s* is related to coordinates *y* and *x* by

$$s^2 = y^2 + x^2 \quad (10.4b)$$

As shown in Fig. 10.5, the first term of the right-hand side of Eq. 10.4a is the equation for a spherical surface of radius *R* = 1/*c*. The subsequent terms represent deformations to the spherical surface, with *A*₂, *A*₄, etc., as the constants of the second, fourth, etc., power deformation terms. Since any number of deformation terms may be included, Eq. 10.4a is quite flexible and can represent some rather extreme aspher-

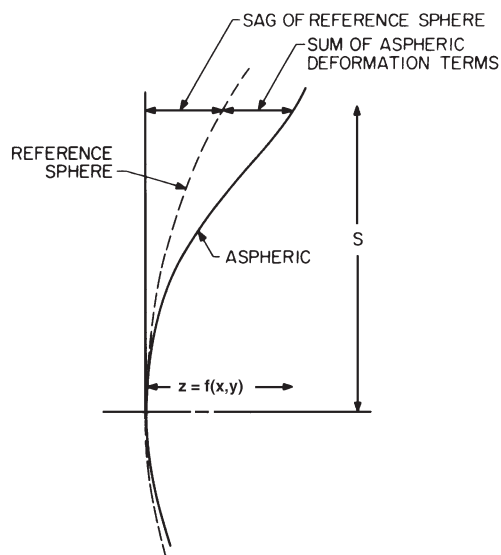


Figure 10.5 Showing the significance of Eq. 10.4a, which defines an aspheric surface by a deformation from a reference spherical surface. The z coordinate of a point on the surface is the sum of the z coordinate of the reference sphere and the sum of all the deformation terms.

ics. Note that Eq. 10.4a is redundant in that the second-order deformation term (A_2s^2) is not necessary to specify the surface, since it can be implicitly included in the curvature c . The importance of the inclusion of this term is that otherwise a large value of c (i.e., a short radius) could be required to describe the surface, and rays which would actually intersect the aspheric surface might not intersect the reference sphere. As can be seen from Example C, if necessary the reference sphere may be a plane.

Aspheric surfaces which are *conic sections* (paraboloid, ellipsoid, hyperboloid) also can be represented by a power series; see Sec. 13.5 for further details.

The difficulty in tracing a ray through an aspheric surface lies in determining the point of intersection of the ray with the aspheric, since this cannot be determined directly. In the method given here, this is accomplished by a series of approximations, which are continued until the error in the approximation is negligible.

The first step is to compute x_0 , y_0 , and z_0 , the intersection coordinates of the ray with the spherical surface (of curvature c) which is usually a fair approximation to the aspheric surface. This is done with Eqs. 10.3c through 10.3j of the preceding section.

Then the z coordinate of the aspheric (\bar{z}_0) corresponding to this distance from the axis is found by substituting $s_0^2 = y_0^2 + x_0^2$ into the equation for the aspheric (10.4a)

$$\bar{z}_0 = f(y_0, x_0) \quad (10.4c)$$

Then compute

$$l_0 = \sqrt{1 - c^2 s_0^2} \tag{10.4d}$$

$$m_0 = -y_0 [c + l_0(2A_2 + 4A_4 s_0^2 + \dots + jA_j s_0^{(j-2)})] \tag{10.4e}$$

$$n_0 = -x_0 [c + l_0(2A_2 + 4A_4 s_0^2 + \dots + jA_j s_0^{(j-2)})] \tag{10.4f}$$

$$G_0 = \frac{l_0 (\bar{z}_0 - z_0)}{(Xl_0 + Ym_0 + Zn_0)} \tag{10.4g}$$

where X , Y , and Z are the direction cosines of the incident ray.

Now an improved approximation to the intersection coordinates is given by

$$x_1 = G_0 X + x_0 \tag{10.4h}$$

$$y_1 = G_0 Y + y_0 \tag{10.4i}$$

$$z_1 = G_0 Z + z_0 \tag{10.4j}$$

The process is sketched in Fig. 10.6.

The approximation process is now repeated (from Eq. 10.4c to 10.4j) until the error is negligible, i.e., until (after k times through the process)

$$z_k = \bar{z}_k \tag{10.4k}$$

to within sufficient accuracy for the purposes of the computation.

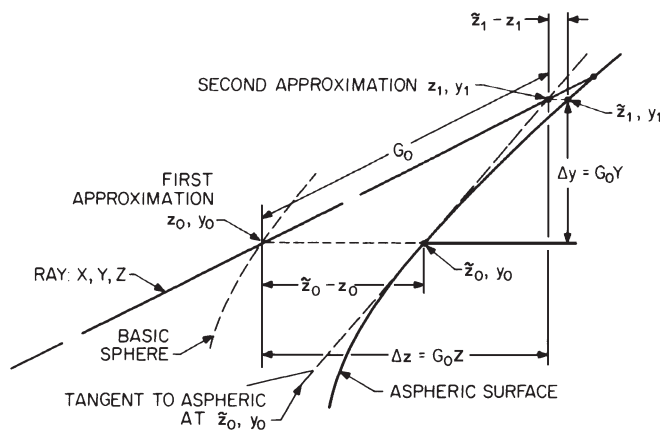


Figure 10.6 Determination of the ray intersection with an aspheric surface. The intersection is found by a convergent series of approximations. Shown here are the relationships involved in finding the first approximation after the intersection with the basic reference sphere has been determined.

The refraction at the surface is carried through with the following equations:

$$P^2 = l_k^2 + m_k^2 + n_k^2 \quad (10.4l)$$

$$F = Zl_k + Ym_k + Xn_k \quad (10.4m)$$

$$F' = \sqrt{P^2 \left(1 - \frac{n^2}{n_1^2}\right) + \frac{n^2}{n_1^2} F^2} \quad (10.4n)$$

$$g = \frac{1}{P^2} \left(F' - \frac{n}{n_1} F \right) \quad (10.4o)$$

$$Z_1 = \frac{n}{n_1} Z + gl_k \quad (10.4p)$$

$$Y_1 = \frac{n}{n_1} Y + gm_k \quad (10.4q)$$

$$X_1 = \frac{n}{n_1} X + gn_k \quad (10.4r)$$

This completes the trace through the aspheric. The spatial intersection coordinates are x_{k_2} , y_{k_2} , and z_{k_2} , and the new direction cosines are X_1 , Y_1 , and Z_1 .

Example C

As a numerical example, let us trace the path of a ray through a paraboloidal mirror. The equation of a paraboloid with vertex at the origin is

$$z = \frac{s^2}{4f}$$

and if we choose a concave mirror with a focal length of -5 , the constants of Eq. 10.4a become $c = 0$, $A_2 = 1/(4f) = -0.05$, and A_4, A_6 , etc., equal zero. Thus

$$z = -0.05s^2 = -0.05(y^2 + x^2)$$

We will place the initial reference plane at the vertex of the parabola and the final reference (image) plane at the focal point. Thus $t = 0$ and $t_1 = f = -5$ (following our usual sign convention for distance after reflections). We will trace the ray striking the reference plane at $z = 0$, $y = 0$, $x = 1.0$ at a direction of $Y = 0.1$, $X = 0$, and (by Eq. 10.3b)

$Z = 0.9949874$. The index of refraction before reflection n equals 1.0 and the index after reflection n_1 will then be -1.0 , again following the convention of reversed signs after reflection.

The computation is indicated in the following tabulation, where the applicable equation number is given in parentheses at each step. The steps indicated by (10.4d) through (10.4c) are repeated top to bottom until $\bar{z}_k = z_k$ to (in this instance) seven places past the decimal. The fact that this example converged in only two cycles despite the fact that $c = 0$ is a poor approximation to our paraboloid, is an indication of the rapidity of convergence of this technique.

Reference surface: $c_0 = 0 \quad t_0 = 0.0 \quad n_0 = 1.0$

Aspheric: $z = -0.05s^2 \quad c_1 = 0 \quad A_2 = -0.05 \quad (A_4, \text{etc.} = 0)$

$$t_1 = -5.0 \quad n_1 = -1.0$$

Image surface: $c_2 = 0$

Given: $z = 0, y = 0, x = +1.0$

$$Z = +0.9949874 \quad Y = +0.10 \quad X = 0.0$$

Since $c = 0$ for the aspheric, it is obvious that $z_0 = z = 0, y_0 = y = 0$, and $x_0 = x = 1.0$. Thus, $\bar{z}_0 = -0.05(y^2+x^2) = -0.05$ (by Eq. 10.4c) and $\bar{z}_0 - z_0 = -0.05$. (The same results can be obtained from Eqs. 10.3c through j)

Intersection of Ray with Aspheric:

(10.4d)	$l_0 = +1.0$	$l_1 = +1.0$
(10.4e)	$m_0 = 0.0$	$m_1 = -0.0005025$
(10.4f)	$n_0 = +0.1$	$n_1 = +0.1$
(10.4g)	$G_0 = -0.0502519$	$G_1 = -0.0000013$
(10.4h)	$z_1 = -0.050$	$z_2 = -0.0500013$
(10.4i)	$y_1 = -0.0050252$	$y_2 = -0.0050253$
(10.4j)	$x_1 = +1.0$	$x_2 = +1.0$
(10.4c)	$\bar{z}_1 = -0.0500013$	$\bar{z}_2 = -0.0500013$
	$\bar{z}_1 - z_1 = -0.0000013$	$\bar{z}_2 - z_2 = 0.0000000$

Refraction:

$$(10.4l) \quad P^2 = +1.0100002$$

$$(10.4m) \quad F = +0.9949372$$

$$(10.4n) \quad F' = +0.9949372$$

$$(10.4o) \quad g = +1.9701722$$

$$(10.4p) \quad Z_1 = +0.09751848$$

$$(10.4q) \quad Y_1 = -0.1009900$$

$$(10.4r) \quad X_1 = +0.1970172$$

$$X_1^2 + Y_1^2 + Z_1^2 = 1.0000001$$

Intersection of Ray with Image Surface:

$$(10.3c) \quad e_1 = -5.0246880$$

$$(10.3d) \quad M_{2z} = +0.0499993$$

$$(10.3e) \quad M_2^2 = +0.2550229$$

$$(10.3f) \quad E_2 = +0.9751848$$

$$(10.3g) \quad L_2 = -5.0759596$$

$$(10.3h) \quad z_2 = 0$$

$$(10.3i) \quad y_2 = +0.5075959$$

$$(10.3j) \quad x_2 = -0.0000513$$

10.6 Coddington's Equations

The tangential and sagittal curvature of field can be determined by a process which is equivalent to tracing paraxial rays along a principal ray, instead of along the axis. In Chap. 3 it was pointed out that the slope of the ray intercept plot was equal to Z_t , the tangential field curvature. This slope *could* be determined by tracing two closely spaced meridional rays and computing

$$Z_t = \frac{H'_1 - H'_2}{\tan U'_2 - \tan U'_1} = \frac{-\Delta H'}{\Delta \tan U'}$$

and a similar process using close sagittal (skew) rays would yield Z_s , the sagittal field curvature.*

Coddington's equations are equivalent to tracing a pair of infinitely close rays, and the formulation has a marked similarity to the paraxial raytracing equations. However, object and image distances as well as surface-to-surface spacings are measured along the principal ray instead of along the axis, and the surface power is modified for the obliquity of the ray.

Figure 10.7 shows a principal ray passing through a surface with sagittal and tangential ray fans originating at an object point and converging to their foci. The distance along the ray from the surface to the focus is symbolized by s and t for the object distance and by s' and t' for the image distance. The sign convention is as usual; if the focus or object point is to the left of the surface, the distance is negative; to the right, positive. In Fig. 10.7, s and t are negative, s' and t' are positive.

*Note that despite the currently almost universal use of z to represent the optical axis, it is still common usage to symbolize field curvature as x_t and x_s .

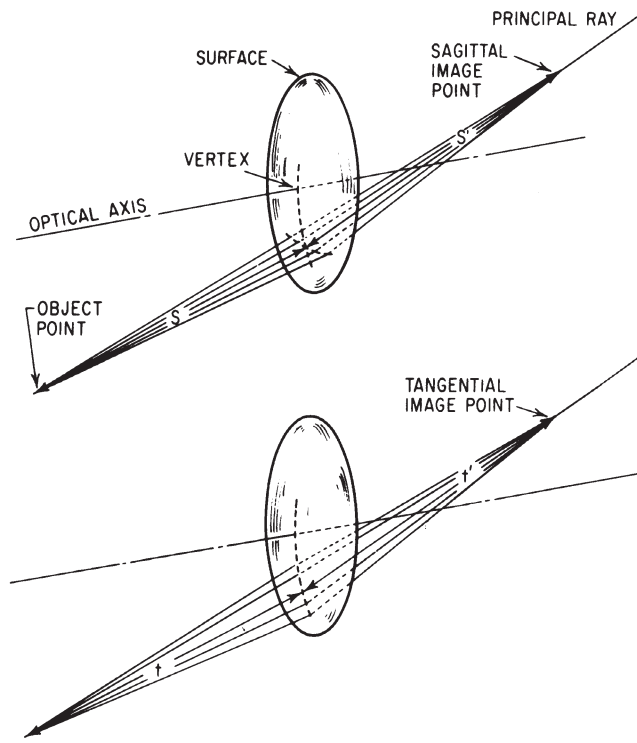


Figure 10.7

The computation is carried out by tracing the principal ray through the system using the meridional formulas of Sec. 10.3, determining the oblique power for each surface by

$$\phi = c (n' \cos I' - n \cos I) \quad (10.5a)$$

and determining the distance (D) from surface to surface along the ray by Eq. 10.2m. The initial values of s and t are determined (Eq. 10.2m is often useful in this regard) and then the focal distances are determined by solving the following equations for s' and t' .

$$\frac{n'}{s'} = \frac{n}{s} + \phi \quad (\text{sagittal}) \quad (10.5b)$$

$$\frac{n' \cos^2 I'}{t'} = \frac{n \cos^2 I}{t} + \phi \quad (\text{tangential}) \quad (10.5c)$$

The values of s and t for the next surface are given by

$$s_2 = s'_1 - D \quad (10.5d)$$

$$t_2 = t'_1 - D \quad (10.5e)$$

where D is the value given by Eq. 10.2m.

The calculation is repeated for each surface of the system; the final values of s' and t' represent the distances along the ray from the last surface to the final foci. The final curvature of field (with respect to a reference plane an axial distance l' from the last surface) can be found from

$$z_s = s' \cos U' + z - l' \quad (10.5f)$$

$$z_t = t' \cos U' + z - l' \quad (10.5g)$$

where z is determined for the last surface by Eq. 10.2l.

The preceding equations are ill-suited for use on an electronic computer, since s and t may be too large for the machine capacity, or too small (so that $1/s$ and $1/t$ become large). The following equations have been developed to avoid this difficulty. They make use of y_s and y_t which are fictional ray heights from the principal ray (analogous to the paraxial ray heights used in Eqs. 10.1) and equally fictional ray slope-index products P_s and P_t with respect to the principal ray.

The calculation is again begun by tracing a principal ray. The opening equations are

$$P_s = \frac{-ny_s}{s} \quad (10.5h)$$

$$P_t = \frac{-ny_t \cos^2 I}{t} \quad (10.5i)$$

where the data refer to the first surface of the system, and y_s and y_t are arbitrarily chosen.

The ray slope-index product after refraction is determined from

$$P'_s = P_s - y_s \phi \quad (10.5j)$$

$$P'_t = P_t - y_t \phi \quad (10.5k)$$

where ϕ is the oblique surface power given by Eq. 10.5a. The "ray height" at the next surface is given by

$$(y_s)_2 = (y_s)_1 + \frac{(P'_s)_1 D}{n'_1} \quad (10.5l)$$

$$(y_t)_2 = \frac{\cos^2 I'_1}{\cos^2 I_2} \left[(y_t)_1 + \frac{(P'_t)_1 D}{n'_1 \cos^2 I'_1} \right] \quad (10.5m)$$

At surface #2, the incident ray slope-index product is given by $P_2 = P'_1$.

This process is repeated for each surface of the system, and the final image distances at the last surface are found from:

$$s' = \frac{-n'y_s}{P'_s} \quad (10.5n)$$

$$t' = \frac{-n'y_t \cos^2 I'}{P'_t} \quad (10.5o)$$

The final curvature of field is found from Eqs. 10.5f and g.

Example D

We will use the meridional ray traced in Example A as the principal ray and trace close sagittal and tangential rays about it, assuming that the object point is at the axial intercept of the ray, i.e., on the axis and 200 mm to the left of the first surface. (From a practical standpoint, this will be equivalent to determining the imagery of the lens when used with a small pinhole diaphragm located 20 mm (radially) away from the axis.)

To find the initial values for s and t , we determine z at the first surface by Eq. 10.2l (using the raytrace data from Example A for the first surface). Then

$$s = t = \frac{l-z}{\cos U} = \frac{-200 - 4.415778}{0.994987} = -205.445587$$

The oblique surface powers are determined from Eq. 10.5a as

$$\phi_1 = +0.02 (1.5 \times 0.942809 - 1.0 \times 0.866025) = + 0.0109638$$

$$\phi_2 = -0.02 (1.0 \times 0.701248 \times -1.5 \times 0.879835) = + 0.0123701$$

Equation 10.2m gives the distance along the ray between surfaces as

$$D = \frac{15.0 - 4.415778 + (-4.177626)}{0.996508} = +6.429045$$

then for the first surface

$$\frac{1.5}{s'} = \frac{1}{-205.445} + 0.0109638$$

$$s' = + 246.0488$$

$$\frac{1.5 (0.942809)^2}{t'} = \frac{0.750}{-205.445} + 0.0109638$$

$$t' = +182.3186$$

We transfer to surface #2 by Eqs. 10.5d and e to get

$$s_2 = +239.6198$$

$$t_2 = +175.8896$$

Then using Eqs. 10.5b and c for the second surface

$$\frac{1}{s'} = \frac{1.5}{239.6198} + 0.0123701$$

$$s'_2 = + 53.6768$$

$$\frac{0.491748}{t'} = \frac{1.161164}{175.8896} + 0.0123701$$

$$t'_2 = + 25.9200$$

By setting l' in Eqs. 10.5f and g equal to +45.6310 (the final intercept of the marginal ray traced in Example A), we find that, with respect to this point,

$$z_s = 49.8086 - 4.1776 - 45.6310 = 0.00$$

$$z_t = 24.0521 - 4.1776 - 45.6310 = -25.7565$$

One may gain an understanding of this rather interesting result by sketching the path of a few rays in a system of the type we have ray-traced, remembering that a simple biconvex lens is afflicted with a large undercorrected spherical aberration. Alternatively, a study of the ray intercept curve for undercorrected spherical (with coordinates rotated to account for the shift of the reference plane to the focus of the marginal ray) will indicate the meaning of the value of z_t found above.

10.7 Aberration Determination

This section will briefly indicate the computational procedures involved in determining the numerical values of the various aberrations discussed in Chap. 3. Since this discussion will be somewhat condensed, the reader may wish to review Chap. 3 at this point.

We will assume that the paraxial focal distance l' (from the vertex of the last surface of the system to the paraxial image) has been determined. It is also useful to predetermine the size and location of the entrance pupil.

Spherical aberration

Trace a marginal meridional ray from the axial intercept of the object (through the edge of the entrance pupil of the system) and determine its final axial intercept L' and/or its intersection height H' in the paraxial focal plane. Then the longitudinal spherical aberration (LA') is given by

$$LA' = L' - l' \quad (10.6a)$$

and the transverse spherical aberration (TA') is given by

$$TA' = H' = -(LA') \tan U' \quad (10.6b)$$

The spherical aberration is overcorrected if the sign of nLA' is positive and undercorrected if the sign is negative.

The zonal spherical aberration is determined by tracing a second ray through the 0.707 zone (i.e., a ray which strikes the entrance pupil at a distance from the axis equal to 0.707 times the distance for the marginal ray). The zonal aberration is found from Eqs. 10.6a and b. Rays may also be traced through other zones of the aperture if a more complete description of the axial correction of the system is required. The customary choice of the $0.707 = \sqrt{0.5}$ zone for zonal rays derives from the fact that, for most systems, the longitudinal spherical can be approximated by

$$LA' = aY^2 + bY^4 \quad (10.6c)$$

where Y is the ray height and a and b are constants. Thus, if the marginal spherical, at a ray height of Y_m , is corrected to zero, the maximum longitudinal zonal aberration occurs at

$$Y = \sqrt{\frac{Y_m^2}{2}} = 0.707Y_m$$

The maximum transverse spherical TA' occurs at

$$Y = \sqrt{0.6Y_m^2} = 0.775Y_m$$

Coma

Three meridional rays are traced from an off-axis object point: a principal ray through the center of the entrance pupil and upper and lower rim rays through the upper and lower edges of the pupil. The final intersection heights of these rays with the paraxial focal plane are determined. Then the tangential coma is given by

$$\text{Coma}_T = H'_A + H'_p + \frac{(H'_A - H'_B)(\tan U'_A - \tan U'_p)}{(\tan U'_B - \tan U'_A)} \quad (10.6d)$$

For most lenses, where the ray slope U' is a smooth uniform function of the ray position in the pupil, the following simplified equation is sufficiently accurate. This can be evaluated when examining a ray intercept plot by connecting the ends of the plot with a straight line and noting the distance from the height of the principal ray intersection to the line.

$$\text{Coma}_T = \frac{H'_A + H'_B}{2} - H'_p$$

where H'_p is the intercept for the principal ray and H'_A and H'_B are the intercepts of the rim rays.

Ordinarily, sagittal coma is very nearly equal to one-third of the tangential coma (especially near the axis). Sagittal coma can be determined by tracing a skew ray through the entrance pupil at $y = 0$, $x =$ the radius of the pupil. Then the displacement of the y intersection coordinate in the image plane from H'_p gives the sagittal coma (note that in this instance the image plane should be the plane of intersection of the upper and lower rim rays, i.e., where $H'_A = H'_B$).

The variation of coma with field angle (or image height) can be determined by repeating the process for another object height. The variation of coma with aperture is found by tracing zonal oblique rays.

OSC

The offense against the (Abbe) sine condition (OSC) is an indication of the amount of coma present in regions near the optical axis. It is determined by tracing a paraxial and a marginal ray from the axial object point and substituting their data into

$$\text{OSC} = \frac{\sin U}{u} \cdot \frac{u'}{\sin U'} \cdot \frac{(l' - l'_p)}{(L' - l'_p)} - 1 \quad (10.6e)$$

where u and u' are the initial and final slopes of the paraxial ray, U and U' are the initial and final slopes for the marginal ray, l' and L' are the final intercept lengths of the paraxial and marginal rays, and l'_p is the final intercept of the principal ray (thus l'_p is the distance from the last surface to the exit pupil). If the object is at infinity, the initial y and Q are substituted for u and $\sin U$ in 10.6e.

For regions near the axis

$$\begin{aligned} \text{Coma}_s &= H' (\text{OSC}) \\ \text{Coma}_t &= 3H' (\text{OSC}) \end{aligned} \quad (10.6f)$$

Distortion

Distortion is found by tracing a meridional principal ray from an off-axis object point through the center of the entrance pupil and determining its intersection height H'_p in the paraxial focal plane. A paraxial principal ray may be traced from the same object point to determine the paraxial image height h' , or the optical invariant I may be used as indicated in Chap. 2.

$$\text{Distortion} = H'_p - h' \quad (10.6g)$$

Distortion is frequently expressed as a percentage of the image height, thus:

$$\text{Percent distortion} = \frac{H'_p - h'}{h'} \times 100 \quad (10.6h)$$

The variation of distortion with image height or field angle is found by repeating the process for several object heights.

Astigmatism and curvature of field

Trace a principal ray from an off-axis object point through the center of the entrance pupil. Then trace close sagittal and tangential rays by Coddington's equations (Sec. 10.6) and determine the final z'_s and z'_t with respect to the paraxial image plane; z'_s and z'_t are then the sagittal and tangential curvature of field for this image point.

Alternatively, a meridional ray from the object point passing through the system close to the principal ray can be traced. Then

$$Z_t = \frac{H'_p - H'}{\tan U' - \tan U'_p} \quad (10.6i)$$

will provide a close approximation to z'_t , since Z'_t approaches z'_t , as the two rays approach each other. A similar procedure with a close skew ray will yield Z'_s .

Since the variation of field curvature with image height is usually of interest, z'_s and z'_t may be determined for additional object heights or field angles and plotted against obliquity.

Note that it is common to refer to the field curvature (z_s and z_t) as x_s and x_t , in conformance with earlier usage when the optical axis was denoted as the x axis.

Chromatic aberration—Axial (or longitudinal)

Paraxial longitudinal chromatic aberration is found by determining the paraxial image points for the longest and shortest wavelengths of light in the spectral bandpass of the system. This is done by determining l' using the indices of refraction associated with one wavelength and then with the other. For visual systems, the long wavelength is usually taken as *C*-light ($\lambda = 0.6563 \mu\text{m}$ hydrogen line) and the short wavelengths as *F*-light ($\lambda = 0.4861 \mu\text{m}$ hydrogen line). The longitudinal chromatic aberration is then

$$\text{LchA}' = l'_F - l'_C \quad (10.6j)$$

The transverse measure of axial chromatic can be found from

$$\text{TAch} = -\text{LchA} \tan U'_K$$

or by calculating the height of the rays in the mid-wavelength focal surface and

$$\text{TAch} = h'_F - h'_C$$

The chromatic aberrations for other zones of the aperture are found by tracing meridional rays from the axial object point for each wavelength and substituting the final axial intercepts into Eq. 10.6j.

The secondary spectrum is found by tracing axial rays in at least three wavelengths—long, middle, and short—and plotting their axial intercepts against wavelength. A numerical value for the secondary spectrum is strictly valid only when the long and short wavelength images are united at a common focus, so that

$$l'_F = l'_C$$

then

$$SS' = l'_d - l'_F = l'_d - l'_C \quad (10.6k)$$

where the subscripts *C*, *d*, and *F* indicate long, middle, and short wavelengths. For visual work, *C*, *F*, and *d* represent the *C* and *F* lines of hydrogen and the helium *d* line at $0.5876 \mu\text{m}$.

The spherochromatism (chromatic variation of spherical aberration) is found by determining the spherical aberration at various wavelengths. Thus, for visual work the spherochromatism would be the spherical in *F* light minus the spherical in *C* light.

Chromatic aberration—Lateral

Lateral chromatic aberration, or chromatic difference of magnification, is determined by tracing a principal ray from an off-axis object point through the center of the entrance pupil in both long and short wavelengths and finding the final intersection heights with the focal plane. Then

$$\text{TchA} = H'_F - H'_C \quad (10.6l)$$

for visual work. Alternatively, the paraxial lateral color can be found by tracing paraxial “principal” rays in two colors and substituting h'_F and h'_C into Eq. 10.6l. The chromatic difference of magnification is given by

$$\text{CDM} = \text{TchA}/h'$$

Lateral chromatic aberration should not be confused with the transverse expression for axial (longitudinal) chromatic aberration, which is given by

$$\text{TAch} = H'_F - H'_C = -(\text{LchA}) \tan U' \quad (10.6m)$$

where the data are derived from rays traced from an object point *on the optical axis*.

Optical path difference (wave-front aberration)

Recalling (from Chap. 1) that a wave front which forms a “perfect” image is spherical in shape and is centered about the image point, it is apparent that the aberration of an image formed by an optical system can be expressed in terms of the departure of the wave front from an ideal spherical wave front. The velocity of light in a medium of index n is given by c/n , where c is the speed of light in vacuum, and the time required for a point on a wave front to travel a distance D through the medium is nD/c . Thus, if a number of rays from an object point are traced through an optical system, and the distances along each ray from surface to surface are computed (by Eqs. 10.2m or 10.4g), including the distance from object point to the first surface, then the points for which $\Sigma nD/c$, or ΣnD , are equal, are points through which the wave front passes at the same instant. A smooth surface through these points is the locus of the wave front.

Referring to Example D, the distance along the ray from the object point to the first surface was computed as 205.446 mm. The distance from surface 1 to surface 2 was $D = 6.429$ mm, and the distance from surface 2 to the axial intercept of the ray was $S'_2 = 53.677$.

If we now multiply each distance by the index (1.0, 1.5, and 1.0, respectively) and sum the products, we find that the *optical path* is

$$\Sigma nD = 268.766$$

The calculation can be repeated for a ray along the axis; the distances are 200 mm, 15 mm, and 45.631, and the optical path along the axis is

$$\Sigma nD = 268.131$$

Since the axial path is shorter by some 0.635 mm, it is apparent that when the wave front reaches this point via the axis, it is still 0.635 mm from the point along the path described by the marginal ray. If we “back up” a bit (a fraction of a nanosecond) to the time when the wave front has just emerged from the lens and construct a reference sphere (or circle) about $L' = 45.631$, it will be apparent that the departure of the wave front from the reference sphere is equal to the difference in the optical paths to the reference sphere. Thus the wave-front aberration or *optical path difference* (OPD) can be found by tracing rays from the object to the surface of a reference sphere centered on the image point and determining

$$\text{OPD} = (\Sigma nD)_A - (\Sigma nD)_B \quad (10.6n)$$

Note that the choice of the reference image point location will have a great effect on the size of the OPD, since a shift of the reference point is equivalent to focusing (in the longitudinal direction) or to scanning the image plane for the point image (when shifting the reference point laterally). In the example cited, a reference sphere constructed about a point 55.57 mm from the last surface would represent a much better “fit” to the wave front, and the OPD about this point would represent (approximately) the minimum obtainable for the aperture represented by this ray.

Although the example cited above showed an OPD of more than 1000 wavelengths of visible light, it should be noted that OPD is usually measured in wavelengths, or fractions thereof. For example, the Rayleigh criterion may be expressed as follows: An image will be “sensibly” perfect if there exists not more than one-quarter wavelength difference in optical path over the wave front with reference to a sphere centered at the selected image point. The numerical precision required to obtain significant results in an OPD calculation is higher than that required for ordinary raytracing. The OPD is customarily determined with respect to a spherical surface (centered about the reference point) with a radius equal to the distance from the exit pupil to the reference point.

10.8 Third-Order Aberrations: Surface Contributions*

If an analytic expression is derived for the transverse aberration of a general ray with respect to a reference ray (i.e., the lateral separation of their intersections in a reference plane), the expression can be broken down into orders, or powers, of the ray parameters. The parameters usually chosen are: (1) the obliquity of the reference ray, and (2) the separation between the two rays at the pupil of the system; they correspond to: (1) image height, and (2) system aperture. The aberrations of the first order turn out to be those which can be eliminated by locating the reference point at the paraxial image. The first-order aberrations are thus defects of focus or image size which vary linearly with aperture or obliquity, such as simple focusing or paraxial chromatic aberration (transverse axial color or lateral color). See Sec. 3.2 and Eqs. 3.1 and 3.2.

The third-order terms correspond to the primary aberrations. The term in y^3 (where y is the semiaperture, or separation of the rays) has no h (image height) component and corresponds to spherical aberration. The term in y^2h corresponds to coma. The term in yh^2 represents the astigmatism and curvature of field, and the term in h^3 is distortion. The portions of the total aberration represented by these terms are called the third-order aberrations.

There will also be terms in y^5 , y^4h , y^3h^2 , y^2h^3 , yh^4 , and h^5 (which are called the fifth-order aberrations), as well as terms in seventh, ninth, and higher exponents. (Note that in European usage, third and fifth order are frequently referred to as primary and secondary aberration). The importance of these aberration contributions diminishes rapidly as the exponent increases, just as in the series expansion for the sine of an angle

$$\sin x = x - \frac{x^3}{3!} + \frac{x^5}{5!} - \frac{x^7}{7!} + \dots$$

The analogy here is quite good, since for optical systems in which the sines of the angles involved can be satisfactorily represented by $\sin x = x$, first-order (paraxial) optics, which are based on just this approximation, are entirely adequate to describe the imagery. For systems with larger angles, more terms of the expansion are necessary to adequately describe the imaging properties, and the third- (or higher-) order aberration contributions must be taken into account.

*D. Feder, "Optical Calculations with Automatic Computing Machines," *J. Opt. Soc. Am.*, vol. 41, pp. 630–636 (1951).

Thus a knowledge of just the paraxial and third-order characteristics frequently yields a fair approximation to the performance of a system which is modest in aperture and angular coverage. In systems where this approximation is poor, the third-order contributions are nonetheless of value. Even in systems where the fifth and higher orders are appreciable, the higher orders tend to change very slowly as the design parameters (radius, spacing, index) are varied, so that, although the first and third orders may be inadequate to fully describe the correction of the system, they are capable of indicating the changes which will be produced by moderate changes in the design parameters. For example, if a parameter change produced a change of Δx in a third-order aberration, one would expect that the change in the total aberration ΔX (as determined by a trigonometric raytrace) would be very nearly equal to Δx , even though the third-order aberration x might be quite different than the trigonometric value X . Further, surfaces which make a large contribution to the third-order aberrations also tend to make a large contribution of the same sign to the higher-order aberrations, and a knowledge of the source of high-order residuals is frequently useful in eliminating them.

The third-order aberration contributions* can be readily calculated from the data of two paraxial rays; an axial ray (from the axial intercept of the object through the rim of the entrance pupil) and a (paraxial) principal ray (from an off-axis object point through the center of the entrance pupil). These rays are traced by Eqs. 10.1a through 10.1g. In the following, the ray data of the axial ray will be symbolized by unsubscripted letters (y, u, i , etc.) and that of the paraxial principal ray by letters with subscript p (y_p, u_p, i_p , etc.).

The optical invariant Inv is determined from the data of the two rays at the first surface, or any convenient surface.

$$Inv = y_p n u - y n u_p = h n'_k u'_k \quad (10.7a)$$

The final image height (i.e., the intersection point of the paraxial "principal" ray in the image plane) is determined from the principal ray or by

$$h = \frac{Inv}{n'_k u'_k} \quad (10.7b)$$

where n'_k and u'_k are the index and slope (of the axial ray) after passing through the last surface of the system.

*The fifth, seventh, etc., orders may also be computed from paraxial raytrace data. Buchdahl develops specific equations by which the higher-order contributions may be calculated. The equations for the fifth-order contributions are very complex and are usually calculated as part of a computer optical software package.

Then the following are evaluated for each surface of the system:

$$i = cy + u \quad (10.7c)$$

$$i_p = cy_p + u_p \quad (10.7d)$$

$$B = \frac{n(n' - n)}{2n' \text{Inv}} y(u' + i) \quad (10.7e)$$

$$B_p = \frac{n(n' - n)}{2n' \text{Inv}} y_p (u'_p + i_p) \quad (10.7f)$$

$$\text{TSC} = Bi^2h \quad (10.7g)$$

$$\text{CC} = Bii_p h \quad (10.7h)$$

$$\text{TAC} = Bi_p^2 h \quad (10.7i)$$

$$\text{TPC} = \frac{-(n - n') ch \text{Inv}}{2nn'} \quad (10.7j)$$

$$\text{DC} = h [B_p i i_p + 1/2(u'_p{}^2 - u_p{}^2)] \quad (10.7k)$$

$$\text{TAchC} = \frac{-yi}{n'_k u'_k} \left(\Delta n - \frac{n}{n'} \Delta n' \right) \quad (10.7l)$$

$$\text{TchC} = \frac{-y i_p}{n'_k u'_k} \left(\Delta n - \frac{n}{n'} \Delta n' \right) \quad (10.7m)$$

As previously, primed symbols refer to quantities after refraction at a surface. Most of the symbols (y , n , u , c) are defined in Sec. 10.2, or immediately above. Those which have not been previously defined are:

B and B_p	Intermediate steps in the calculation.
i	The paraxial angle of incidence.
Δn	The dispersion of the medium, equal to the difference between the index of refraction for the short wavelength and long wavelength. For visual work, $\Delta n = n_F - n_C$, or $\Delta n = (n - 1)/V$.
Inv	The optical invariant

The third-order aberration contributions of the individual surfaces are given by Eqs. 10.7g through 10.7m, where

TSC	is the transverse third-order spherical aberration contribution.
CC	is the sagittal third-order coma contribution.
3CC	is the tangential third-order coma contribution.

TAC	is the transverse third-order astigmatism contribution.
TPC	is the transverse third-order Petzval contribution.
DC	is the third-order distortion.
TAchC	is the paraxial transverse axial chromatic aberration contribution.
TchC	is the paraxial lateral chromatic aberration contribution.

Note that TAchC and TchC are first-order aberrations; since they are customarily computed at the same time as the third-order aberrations, the equations are presented here.

The longitudinal values of the contributions may be obtained by dividing the transverse values by u'_k , the final slope of the axial ray, thus

$$\begin{aligned}
 \text{SC} &= \frac{-\text{TSC}}{u'_k} \\
 \text{AC} &= \frac{-\text{TAC}}{u'_k} \\
 \text{PC} &= \frac{-\text{TPC}}{u'_k} \\
 \text{LAchC} &= \frac{-\text{TAchC}}{u'_k}
 \end{aligned}
 \tag{10.7n}$$

The *Seidel coefficients* can be obtained by multiplying the transverse third-order contributions or sums by $(-2n'_k u'_k)$. Thus

$$\begin{aligned}
 \text{S1} &= -\text{TSC} (2n'_k u'_k) \\
 \text{S2} &= -\text{CC} (2n'_k u'_k) \\
 \text{S3} &= -\text{TAC} (2n'_k u'_k) \\
 \text{S4} &= -\text{TPC} (2n'_k u'_k) \\
 \text{S5} &= -\text{DC} (2n'_k u'_k)
 \end{aligned}$$

The third-order aberrations at the final image are obtained by adding together the contributions of all the surfaces to get ΣTSC , ΣCC , ΣTAC , etc. These contribution sums are as follows:

ΣTSC	is the third-order transverse spherical aberration.
ΣSC	is the third-order longitudinal spherical aberration.
ΣCC	is the third-order sagittal coma.
$3\Sigma\text{CC}$	is the third-order tangential coma.

ΣTAC	is the third-order transverse astigmatism.
ΣAC	is the third-order longitudinal astigmatism.
ΣTPC	is the third-order transverse Petzval sum.
ΣPC	is the third-order longitudinal Petzval sum.
ΣDC	is the third-order distortion.
ΣTAchC	is the first-order transverse axial color.
ΣLchC	is the first-order longitudinal axial color.
ΣTchC	is the first-order lateral color.

To the extent that the first- and third-order aberrations approximate the complete aberration expansions, the following relationships are valid:

$$\begin{aligned}\Sigma\text{SC} &\approx L' - l' && \text{(spherical)} \\ 3\Sigma\text{CC} &\approx \frac{1}{2}(H'_A + H'_B) - H'_p && \text{(tangential coma)} \\ z_s &\approx \Sigma\text{PC} + \Sigma\text{AC} && \text{(sag. curvature of field, } x_s) \\ z_t &\approx \Sigma\text{PC} + 3\Sigma\text{AC} && \text{(tan. curvature of field, } x_t) \\ \rho &= \frac{h^2}{2\Sigma\text{PC}} && \text{(Petzval radius of curvature)} \\ \frac{100\Sigma\text{DC}}{h} &\approx \text{percentage distortion} \\ \Sigma\text{LAchC} &\approx l'_F - l'_C && \text{(axial color)} \\ \Sigma\text{TchC} &\approx h'_F - h'_C && \text{(lateral color)}\end{aligned}$$

Contributions from aspheric surfaces

For the purposes of computing the third-order contributions, we can assume that the aspheric surface is represented by a power series in s^2

$$z = \frac{1}{2}C_e s^2 + (\frac{1}{8}C_e^3 + K) s^4 + \dots \quad (10.7o)$$

in which the terms in s^6 and higher may be neglected. For aspheric surfaces given in the form of Eq. 10.4a, the equivalent curvature C_e and equivalent fourth-order deformation constant K may be determined from

$$C_e = c + 2A_2 \quad (10.7p)$$

$$K = A_4 - \frac{A_2}{4} (4A_2^2 + 6cA_2 + 3c^2) \quad (10.7q)$$

where c , A_2 , and A_4 , are the curvature and second- and fourth-order deformation terms, respectively, of Eq. 10.4a. Note that if A_2 is zero, $C_e = c$ and $K = A_4$; see Sec. 13.5 for conics, where $A_4 = \kappa/8R^3$.

The aspheric surface contributions are determined by first computing the contributions for the equivalent spherical surface C_e using Eqs. 10.7g through m. Then the contributions due to the equivalent fourth-order deformation constant K are computed by the following equations and added to those of the equivalent spherical surface to obtain the total third-order aberration contribution of the aspheric surface.

$$W = \frac{4K(n' - n)}{\text{Inv}} \quad (10.7r)$$

$$\text{TSC}_a = Wy^4h \quad (10.7s)$$

$$\text{CC}_a = Wy^3y_p h \quad (10.7t)$$

$$\text{TAC}_a = Wy^2y_p^2h \quad (10.7u)$$

$$\text{TPC}_a = 0 \quad (10.7v)$$

$$\text{DC}_a = Wyy_p^3h \quad (10.7w)$$

$$\text{TAchC}_a = 0 \quad (10.7x)$$

$$\text{TchC}_a = 0 \quad (10.7y)$$

It is worth noting that if the aspheric surface is located at the aperture stop (or at a pupil), then $y_p = 0$, and the only third-order aberration that is affected by the aspheric term is spherical aberration. The Schmidt camera makes use of this by placing its aspheric corrector plate at the stop so that only the spherical aberration of the spherical mirror is affected by the plate. Conversely, if an aspheric is expected to affect coma, astigmatism, or distortion, it must be located a significant distance from the stop.

Example E

We shall determine the third-order surface contributions of the simple biconvex lens of Example A. We have already traced an axial paraxial ray in this example; we shall add a paraxial principal ray from an object point 20 mm below the axis and assume that the entrance pupil is at the first surface. Thus the starting data for this ray will be $y_p = 0$ and $u_p = -0.1$. We shall also assume that the lens is of crown glass with a V -value of 62.5 (and therefore $\Delta n = 0.008$).

<i>c</i>		+0.02		-0.02	
<i>t</i>			15.0		
<i>n</i>		1.0	1.5		1.0
<i>y</i>	by 10.1d		+20.0	+19.0	
<i>u</i>	by 10.1c	+0.1	-0.066667		-0.29
<i>i</i>	by 10.7c		+0.5	-0.446667	
					by 10.1f <i>l'</i> =65.517241
<i>y_p</i>	by 10.1d		0	+1.0	
<i>u_p</i>	by 10.1c	+0.1	+0.066667		+0.09
<i>i_p</i>	by 10.7d		+0.1	+0.046667	
					by 10.1g <i>h'</i> =6.896552
	by 10.7a	Inv=-2.0			
	by 10.7b	<i>h'</i> = 6.896552			
B	by 10.7e		-0.722222	-2.624375	
B _p	by 10.7f		0.0	+0.025625	
TSC	by 10.7g		-1.245211	-3.610979	ΣTSC = -4.856190
SC	by 10.7n		-4.294	-12.452	ΣSC = -16.745
CC	by 10.7h		-0.249042	+0.377266	ΣCC = +0.128224
TAC	by 10.7i		-0.049808	-0.039416	ΣTAC = -0.089224
AC	by 10.7n		-0.1717	-0.1359	ΣAC = -0.3077
TPC	by 10.7j		-0.045977	-0.045977	ΣTPC = -0.091954
PC	by 10.7n		-0.1585	-0.1585	ΣPC = -0.3171
DC	by 10.7k		-0.019157	+0.008922	ΣDC = -0.010235
TAchC	by 10.7l		-0.183908	-0.234115	ΣTAchC = -0.418023
LchC	by 10.7n		-0.6342	-0.8073	ΣLchC = -1.4415
TchC	by 10.7m		-0.036782	+0.024460	ΣTchC = -0.012322

Example F

To illustrate the use of the aspheric third-order contribution formulas, we shall demonstrate that the third-order spherical of a paraboloidal mirror is equal to zero for an infinitely distant object. The equation for a paraboloid is simply $z = s^2/4f$, and in terms of Eq. 10.4a, $c = 0$, $A_2 = 1/(4f)$ and the higher-order constants (A_4 , A_6 , etc.) are all zero. Thus, by Eqs. 10.7p, q, and r, we find that

$$C_e = \frac{1}{2f}$$

$$K = \frac{-1}{64f^3}$$

$$W = \frac{-8K}{\text{Inv}} = \frac{+1}{8f^3 \text{Inv}}$$

remembering that for a mirror in air $n = 1.0$ and $n' = -1.0$. Then Eq. 10.7s gives the contribution of the equivalent deformation constant as

$$\text{TSC}_a = + \frac{y^4 h}{8f^3 \text{Inv}}$$

For an infinite object distance, the axial ray has a slope $u = 0$; Eq. 10.1c gives us (using $C_e u' = -y/f$ and Eq. 10.7c yields $i = y/2f$). Substituting these values into Eq. 10.7e, we get

$$\begin{aligned} B &= \frac{(1.0)(-1.0 - 1.0)}{2(-1.0) \text{Inv}} y \left(\frac{-y}{f} + \frac{y}{2f} \right) \\ &= \frac{-y^2}{2f \text{Inv}} \end{aligned}$$

Now Eq. 10.7g gives the spherical aberration contribution of the equivalent sphere as

$$\begin{aligned} \text{TSC} &= \frac{-y^2}{2f \text{Inv}} \left(\frac{y}{2f} \right)^2 h \\ &= \frac{-y^4 h}{8f^3 \text{Inv}} \end{aligned}$$

The contribution of the paraboloid mirror is given by the sum of TSC and TSC_a ; since they are equal in magnitude and opposite in sign, the sum is zero.

Note that the demonstration did not specify that the paraboloid was concave (the more usual case); a convex paraboloid is equally free of spherical when used in this manner. And although we assumed the reflector to be in air for convenience, had we carried the indices $n' = -n$ through the calculation, the result would have been the same.

10.9 Third-Order Aberrations: Thin Lenses; Stop Shift Equations

When the elements of an optical system are relatively thin, it is frequently convenient to assume that their thickness is zero. As we have previously noted, this assumption results in simplified approximate expressions for element focal lengths, which are nonetheless quite useful for rough preliminary calculations. This approximation can be applied to third-order aberration calculations; the results form a very useful tool for preliminary analytical optical system design. The following equations may be derived by application of the equations of the preceding section to a lens element of zero thickness.

The thin-lens third-order aberrations are found by tracing an axial and a principal ray through the system of thin lenses, in the manner outlined in Chap. 2. The equations used are

$$u' = u - y\phi \quad (10.8a)$$

$$y_2 = y_1 + du'_1 \quad (10.8b)$$

where u and u' are the ray slopes before and after refraction by the element, ϕ is the element power (reciprocal focal length), y is the height at which the ray strikes the element, and d is the spacing between adjacent elements.

From Chap. 2 we also recall that the power of a thin element is given by

$$\begin{aligned} \phi &= 1/f \\ &= (n - 1)(c_1 - c_2) \\ &= (n - 1)c \end{aligned} \quad (10.8c)$$

where $c = c_1 - c_2$ and c_1 and c_2 are the curvatures (reciprocal radii) of the first and second surfaces of the element.

After tracing the axial and “principal” rays through the system, the following are computed for each element

$$v = \frac{u}{y} \left(\text{or } v' = \frac{u'}{y} \right) \quad (10.8d)$$

$$Q = \frac{y_p}{y} \quad (10.8e)$$

where u and y are taken from the data of the axial ray and y_p is from the principal ray data.

Then the aberration contributions may be determined from the *stop shift equations*:

$$\text{TSC}^* = \text{TSC} \quad (10.8f)$$

$$\text{CC}^* = \text{CC} + Q \cdot \text{TSC} \quad (10.8g)$$

$$\text{TAC}^* = \text{TAC} + 2Q \cdot \text{CC} + Q^2 \text{TSC} \quad (10.8h)$$

$$\text{TPC}^* = \text{TPC} \quad (10.8i)$$

$$\text{DC}^* = \text{DC} + Q(\text{TPC} + 3\text{TAC}) + 3Q^2 \text{CC} + Q^3 \text{TSC} \quad (10.8j)$$

$$\text{TAchC}^* = \text{TAchC} \quad (10.8k)$$

$$\text{TchC}^* = \text{TchC} + Q \cdot \text{TAchC} \quad (10.8l)$$

The starred terms are the contributions from an element which is not at the stop—that is, one for which $y_p \neq 0$. The unstarred terms are the contributions from the element when it is in contact with the stop (and $y_p = 0$) and are given by the following equations:

$$\begin{aligned} \text{TSC} &= \frac{y^4}{u'_k} (G_1c^3 - G_2c^2c_1 - G_3c^2v + G_4cc_1^2 + G_5cc_1v + G_6cv^2) \\ &= \frac{y^4}{u'_k} (G_1c^3 + G_2c^2c_2 + G_3c^2v' + G_4cc_2^2 + G_5cc_2v' + G_6cv'^2) \end{aligned} \quad (10.8m)$$

$$\begin{aligned} \text{CC} &= -hy^2(0.25G_5cc_1 + G_7cv - G_8c^2) \\ &= -hy^2(0.25G_5cc_2 + G_7cv' + G_8c^2) \end{aligned} \quad (10.8n)$$

$$\text{TAC} = \frac{h^2\phi u'_k}{2} \quad (10.8o)$$

$$\text{TPC} = \frac{h^2\phi u'_k}{2n} = \frac{\text{TAC}}{n} \quad (10.8p)$$

$$\text{DC} = 0 \quad (10.8q)$$

$$\text{TAchC} = \frac{y^2\phi}{Vu'_k} \quad (10.8r)$$

$$\text{TchC} = 0 \quad (10.8s)$$

$$\text{TSchC} = \frac{y^2\phi P}{Vu'_k} \quad (10.8t)$$

The symbols in the preceding have the following meanings:

u'_k is the final slope of the axial ray (at the image).

h is the image height (the intersection of the “principal” ray with the image plane).

V is the Abbe V -number of the lens material, equal to $(n_d - 1)/(n_F - n_C)$.

P is the partial dispersion of the lens material, equal to $(n_d - n_C)/(n_F - n_C)$.

G_1 through G_8 are functions of the lens material index, listed below.

TSC, CC, TAC, DC, TPC, TAchC, and TchC have the same meanings as in Sec. 10.8.

TSchC is the transverse secondary spectrum contribution, equal to $(l'_d - l'_c)(-u'_k)$.

The transverse aberrations may be converted to longitudinal measure by dividing by $(-u'_k)$ per Eq. 10.7n, as follows:

$$\begin{aligned} \text{SC} &= \frac{-\text{TSC}}{u'_k} \\ \text{AC} &= \frac{-\text{TAC}}{u'_k} \\ \text{PC} &= \frac{-\text{TPC}}{u'_k} \\ \text{LchC} &= \frac{-\text{TAchC}}{u'_k} \\ \text{SchC} &= \frac{-\text{TSchC}}{u'_k} \end{aligned}$$

The relations between the thin-lens contributions and the various measures of the aberrations are the same as indicated in Sec. 10.8.

$$\begin{aligned} G_1 &= \frac{n^2(n-1)}{2} & G_5 &= \frac{2(n+1)(n-1)}{n} \\ G_2 &= \frac{(2n+1)(n-1)}{2} & G_6 &= \frac{(3n+2)(n-1)}{2n} \\ G_3 &= \frac{(3n+1)(n-1)}{2} & G_7 &= \frac{(2n+1)(n-1)}{2n} \\ G_4 &= \frac{(n+2)(n-1)}{2n} & G_8 &= \frac{n(n-1)}{2} \end{aligned} \quad (10.8u)$$

The contributions, TSC*, CC*, etc., are determined for each element in the system. The individual contributions are then added to get ΣTSC^* , ΣCC^* , etc., and, to the extent that (1) the thin-lens fiction is valid, and (2) the third-order aberrations represent the total aberration of the system,

$$\begin{aligned} \Sigma\text{SC} &\approx L' - l' \\ \Sigma\text{CC}^* &\approx \text{coma}_S \approx \frac{1}{3}\text{coma}_T \\ \Sigma\text{PC}^* + \Sigma\text{AC}^* &\approx x_s \quad (\text{sagittal field curvature}) \\ \Sigma\text{PC}^* + 3\Sigma\text{AC}^* &\approx x_t \quad (\text{tangential field curvature}) \\ \frac{1}{\Sigma\frac{\phi}{n}} &= -\rho = \text{Petzval radius} \end{aligned}$$

$$\frac{100 \Sigma DC^*}{h} \approx \text{percentage distortion}$$

$$\Sigma LchC = l'_F - l'_C$$

$$\Sigma TchC^* = h_F - h_C$$

$$\Sigma SchC = l'_d - l'_C$$

The thin-lens third-order aberration expressions (which are frequently called G -sums) can be used with the specific data of an optical system to determine the (approximate) aberration values. Another usage is in design work where the curvatures and/or spacings and powers of the elements are to be determined in such a way that the aberration values are equal to some desired set of values, as will be evident in Chap. 12. For aspheric surfaced lenses, the contributions from the asphericity are calculated (by Eqs. 10.7r through 10.7y) and added to the contributions calculated for spherical surfaced lenses.

Equations 10.8f to 10.8l are called *stop shift equations*. They may also be applied to the *surface* contributions (from Eqs. 10.7) to determine the third-order aberrations for a new, or changed, stop position by setting

$$Q = \frac{(y_p^* - y_p)}{y}$$

where y_p^* is the ray height of the “new” principal ray (i.e., after the stop is shifted) and y_p and y are as indicated in Sec. 10.8. Note that Q is an invariant; thus the values for y_p^* , y_p , and y may be taken at *any* convenient surface. When the equations are used this way the unstarred terms (SC, CC, etc.) refer to the aberrations with the stop in the original position, while the starred terms (SC*, CC*, etc.) refer to the aberrations with the stop in the new position. Another consequence of the invariant nature of this definition of Q is the fact that the stop shift may be applied to either the individual surface contributions or to the contribution sums of the entire system or any portion thereof.

The implications of the stop shift equations (Eqs. 10.8f through l) are worthy of note. If *all* the third-order aberrations are corrected for a given stop position, then moving the stop will not change them. Similarly, if there is no spherical, the coma is not affected by a stop shift. This is the case with the paraboloid mirror which, because it has no spherical aberration, has the same amount of coma regardless of where the stop is placed. But because it has coma, the astigmatism is a function of the stop position.

Example G

We will repeat Example E, assuming that the lens is thin. Since $c_1 = +0.02$ and $c_2 = -0.02$, the power of the thin lens is $\phi = (1.5-1) \times (+0.02+0.02) = +0.02$. For the axial ray $u = +0.1$ and $y = 20$; Eq. 10.8a gives $u' = -0.3$, and, since there is only one element in the "system," $u' = u'_k = -0.3$. The final image distance is $-20/(-0.3) = 66.6$ mm and the image height corresponding to an object height of -20 mm can be determined by $h' = hu/u' = +6.66$ mm, or by tracing a paraxial principal ray.

Applying Eqs. 10.8u, we find the G -functions corresponding to $n = 1.5$ to be

$$\begin{array}{ll} G_1 = 0.5625 & G_5 = 1.666\dots \\ G_2 = 1.0 & G_6 = 1.08333\dots \\ G_3 = 1.375 & G_7 = 0.666\dots \\ G_4 = 0.5833\dots & G_8 = 0.375 \end{array}$$

Thus we have the data (tabulated below for convenience) necessary to determine the "stop in contact" aberrations.

$$\begin{array}{lll} y = +20 & y^2 = +400 & y^4 = +160,000 = 16 \times 10^4 \\ u'_k = -0.3 & u'_k{}^2 = +0.09 & \\ c = +0.04 & c^2 = 16 \times 10^{-4} & c^3 = 64 \times 10^{-6} \\ c_1 = +0.02 & c_1^2 = 4 \times 10^{-4} & \\ v = +0.005 & v^2 = +25 \times 10^{-6} & \\ h = +6.66\dots & h^2 = 44.44\dots & \\ V = 62.5 & & \\ \phi = +0.02 & & \end{array}$$

We will use the first surface versions of Eqs. 10.8m and n; the second surface versions (data in c_2 and v') are primarily for use in analytical work with cemented doublets where it is desirable to express the aberration of the doublet as a function of the curvature of the cemented surface.

$$\begin{aligned} \text{TSC} = \frac{16 \times 10^4}{-0.3} [& 0.5625 \times 64 \times 10^{-6} - 1.0 \times 16 \times 10^{-4} \times 0.02 \\ & - 1.375 \times 16 \times 10^{-4} (+ 0.005) + 0.5833 \times 0.04 \times 4 \times 10^{-4} \\ & + 1.666 \times 0.04 \times 0.02 (+ 0.005) + 1.0833 \times 0.04 \times 25 \times 10^{-6}] \end{aligned}$$

$$\begin{aligned}
\text{TSC} &= -5.333 \times 10^5 [+36 \times 10^{-6} - 32 \times 10^{-6} - 11 \times 10^{-6}] \\
&\quad + 9.33 \times 10^{-6} + 6.66 \times 10^{-6} + 1.0833 \times 10^{-6}] \\
&= -5.333 \times 10^5 [+10.0833 \times 10^{-6}] \\
&= -5.3777\dots
\end{aligned}$$

$$\begin{aligned}
\text{CC} &= -6.666 \times 400 [0.25 \times 1.666 \times 0.04 \times 0.02 \\
&\quad + 0.666 \times 0.04 (+0.005) - 0.375 \times 16 \times 10^{-4}] \\
&= -2.666 \times 10^3 [+3.33 \times 10^{-4} + 1.333 \times 10^{-4} - 6 \times 10^{-4}] \\
&= -2.666 \times 10^3 [-1.333 \times 10^{-4}] \\
&= +0.3555\dots
\end{aligned}$$

$$\begin{aligned}
\text{TAC} &= \frac{44.44 \times 0.02 \times (-0.3)}{2} \\
&= -0.1333\dots
\end{aligned}$$

$$\begin{aligned}
\text{TPC} &= \frac{44.44 \times 0.02 \times (-0.3)}{2 \times 1.5} \\
&= -0.0888\dots
\end{aligned}$$

$$\text{DC} = 0.0$$

$$\begin{aligned}
\text{TAchC} &= \frac{400 \times 0.02}{62.5 \times (-0.3)} \\
&= -0.42666\dots
\end{aligned}$$

$$\text{TchC} = 0.0$$

The above are the third-order aberrations of our thin lens with the stop (pupil) at the lens; these results may be compared with Example E (where the stop was at the first surface).

However, let us assume that the stop is 50 mm to the left of the lens. With the object height of -20 mm as before, this gives $u_p = +20/150 = +0.13333$ and $y_p = -20 + 200(+0.1333) = +6.666$. Thus, Eq. 10.8e gives $Q = +0.333$ and we can determine the aberrations of the lens under these conditions from Eqs. 10.8f through l.

$$\text{TSC}^* = -5.3777\dots$$

$$\begin{aligned}
\text{CC}^* &= +0.3555 + 0.333(-5.3777) \\
&= -1.4370
\end{aligned}$$

$$\begin{aligned} \text{TAC}^* &= -0.1333 + 2(0.333)(0.3555) + (-5.3777)(0.333)(0.333) \\ &= -0.4938 \end{aligned}$$

$$\text{TPC}^* = -0.0888$$

$$\begin{aligned} \text{DC}^* &= 0 + (0.333)(-0.0888 - 0.4) + 3(0.333)(0.333)(0.3555) \\ &\quad + (0.333)(0.333)(0.333)(-5.3777) \\ &= -0.1629629 + 0.1185185 - 0.1991767 \\ &= -0.2436 \end{aligned}$$

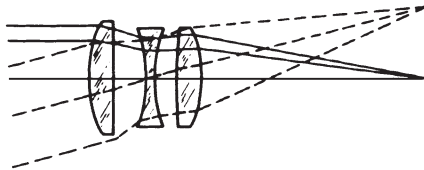
$$\text{TAchC}^* = -0.42666\dots$$

$$\begin{aligned} \text{TchC}^* &= 0 + 0.333(-0.42666) \\ &= -0.1422 \end{aligned}$$

Example H

As a final example for this chapter, we present a raytrace analysis of an air-spaced photographic triplet lens. The constructional data shown in Fig. 10.8 are taken from K. Pestrecov's U.S. Patent No. 2,453,260 (1948). Although the data are for a focal length of 100, this lens is designed for use as an 8- or 16-mm movie camera objective of short focal length (i.e., $f = 13\text{--}26$ mm).

The analysis is begun by determining the size and position of the entrance pupil. The patent gives a speed of $f/2.7$; thus the pupil diameter is 37 units, and, if we assume the stop to be at R_4 , the apparent position of the pupil is 25 units to the right of R_1 . For an object at infinity, the paraxial rays necessary for the third-order aberration calculation



$R_1 = +40.94$	$t_1 = 8.74$	$n_D = 1.617$	$V = 55.0$
$R_2 = \text{Plano}$	$t_2 = 11.05$		
$R_3 = -55.65$	$t_3 = 2.78$	$n_D = 1.649$	$V = 33.8$
$R_4 = +39.75$	$t_4 = 7.63$		
$R_5 = +107.56$	$t_5 = 9.54$	$n_D = 1.617$	$V = 55.0$
$R_6 = -43.33$			

Figure 10.8 Section drawing and constructional data for a triplet photographic objective ($f/2.7$, focal length 100) from U.S. Patent No. 2,453,260 (1948-Pestrecov).

are represented by $u = 0$, $y = 18.5$, $u_p = +0.25$, and $y_p = -6.3$. The results are

$$\begin{aligned} \text{efl} &= 100.0 & \Sigma\text{CC} &= +0.0017 & \Sigma\text{DC} &= +0.057 \\ \text{bfl} &= 79.34 & \Sigma\text{TAC} &= +0.070 & \Sigma\text{TachC} &= -0.059 \\ \Sigma\text{TSC} &= -0.422 & \Sigma\text{TPC} &= -0.272 & \Sigma\text{TchC} &= +0.021 \end{aligned}$$

Next, meridional rays are traced for the axial bundle ($U = 0$) in C , D , and F light. For the marginal ray $Q_1 = 18.5$ and for the zonal ray $Q_1 = 13.1$. The results are plotted in Fig. 10.9; plot A shows transverse measure and plot F longitudinal measure.

Principal rays are traced at several obliquities through the center of the pupil (so that $-Q/\sin U = l_{pr} = 25.0$) and Coddington's equations

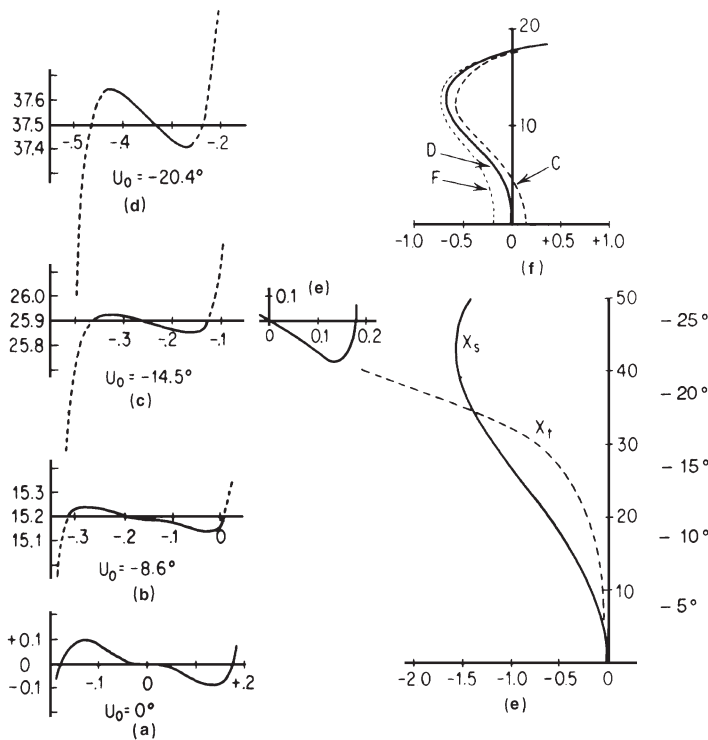


Figure 10.9 Aberration plots of $f/2.7$ triplet (see Fig. 10.8 for constructional data). Plots (a), (b), (c), (d) are meridional ray intercept curves with H (in the paraxial focal plane) as ordinates and $\tan U_6$ as abscissa. The dashed portions indicate rays cut off by vignetting. Plot (e) is one-half of a sagittal (skew) fan, with x as ordinate. Plot (f) shows the longitudinal spherical aberration (abscissa) as a function of the entering ray height. Plot (g) shows sagittal and tangential field curvature (abscissa) as a function of the final image height.

are applied to determine the field curvature, which is shown in plot G of Fig. 10.9.

To compute the data for the ray intercept curves, a fan of meridional rays was traced at each obliquity. The starting data were chosen so that one ray (principal) passed through the center of the pupil and pairs of rays passed through the rims ($Y = \pm 18.5$), the 75 percent zones ($Y = \pm 13.875$) and the 50 percent zones ($Y = \pm 9.25$). For example, the starting values for Q for the bundle at $+14.5^\circ$ ($\sin U_1 = +0.25$) were -6.25 for the principal ray and $+11.662548$ and -24.162548 for the rays through the pupil rim. (These three rays are shown as dashed lines in Fig. 10.8). The seven final values of H' (in the paraxial focal plane 79.3357 to the right of R_6) are plotted against $\tan U'_6$. Note also that the slope of the plot through the point representing the principal ray is equal to $Z_T(Z_T = -dH'/d \tan U' = X_p)$.

A sketch of the system with the rays drawn in (as in Fig. 10.8) will indicate which rays do not get through the lens; in Fig. 10.9, we indicate this by dashing the vignetted portion of the ray intercept curve. We assumed a clear aperture of 37 at R_1 and 32 at R_6 .

A sagittal fan of three rays was traced with pupil intersections $z = 0$, $y = 0$, and $x = 18.5$, 13.875 , and 9.25 . The final values of x in the image plane are plotted in Fig. 10.9e against the final ray direction cosine Z . The slope of this curve through the point $(0, 0)$ can be obtained from $z_s = -dx/d \tan U_z = x_s$.

A very minimal raytrace analysis might consist of the following:

1. Paraxial trace and third-order aberrations.
2. Marginal and zonal axial rays in three colors.
3. Coddington's trace at full field and 0.7 field.
4. Tangential fan of five rays (including the principal ray used in 3) at full and 0.7 field, at least one fan in three colors.

From this, one cannot only obtain the aberration plots of Fig. 10.9, but a number of other relationships such as:

Variation of: Spherical with obliquity
 Coma with obliquity
 Coma with aperture
 Distortion with obliquity
 Lateral color with obliquity

The completeness with which one must analyze a system varies greatly. Systems of large aperture or field angle will require a more complete analysis. Systems of small aperture and field may not even

require a “zonal” analysis. If one is familiar with the general type of system under analysis, frequently the third-order aberrations plus a few carefully selected rays will yield an adequate picture of the system performance. Of course, a modern computer program delivers a complete analysis so easily that trying to minimize the amount of raytracing is not a very profitable way to spend one’s time.

Bibliography

Note: Titles preceded by an asterisk are out of print.

Buchdahl, H., *Optical Aberration Coefficients*, Oxford, 1954.

*Conrady, A., *Applied Optics and Optical Design*, Oxford, 1929. (This and vol. 2 also were published by Dover, New York.)

Herzberger, M., *Modern Geometrical Optics*, New York, Interscience, 1958.

Kingslake, R., *Optical System Design*, San Diego, Academic, 1983.

Smith, W., in W. Driscoll (ed.), *Handbook of Optics*, New York, McGraw-Hill, 1978.

Smith, W., in Wolfe and Zissis (ed.), *The Infrared Handbook*, Washington, Office of Naval Research, 1985.

*Welford, W., *Aberrations of the Symmetrical Optical System*, New York, Academic, 1974.

Exercises

Numerical exercises in optical computation tend to be excessively laborious, and when mistakes are made, the result is more often discouragement than enlightenment. Therefore, we suggest that the reader desirous of only a moderate amount of adventure scale the dimensional data of the numerical examples contained in this chapter by a convenient factor, say $0.5\times$ or $2\times$, and repeat the computations independently.

For those who wish a bit more exercise, the following problems are based on the data of Example H and Fig. 10.8. The index of refraction data are as follows:

n_D	$n_F - n_C$	n_C	n_F
1.617	0.01123	1.61370	1.62493
1.649	0.01920	1.64355	1.66275

1 Determine the third-order aberrations. The initial ray data and answers are given in the second paragraph of Example H.

2 Trace principal rays in D , C , and F light with starting data $Q = -6.25$, $\sin U = +0.25$.

ANSWER: $H'_D = 25.8793$, $H'_C = 25.8720$, $H'_F = 25.8966$

3 Trace close sagittal and tangential rays from an infinitely distant object by Coddington's equations, using the D light principal ray of Exercise 2.

ANSWER: $Z_s (= X_s) = -0.9528$; $Z_t (= X_t) = -0.4521$

4 Trace a sagittal skew ray at obliquity $\sin U = +0.25$ (direction cosine $Y = +0.25$) through the rim of the 37-diameter entrance pupil located 25 to the right of R_1 .

ANSWER: $Z = 0.94805$ $Y = 0.25941$ $X = -0.18416$
 $z = 0$ $y = 25.8657$ $x = 0.0757$

5 Sketch the appearance of the ray intercept curves of Fig. 10.9 (A , B , C , D , and E) in a plane 78.94 from R_6 (i.e., 0.4 inside the paraxial focus). Note that this does not require additional raytracing.